Available online at www.sciencedirect.com

ScienceDirect

Energy Procedia 158 (2019) 809–815

Energy Procedia

www.elsevier.com/locate/procedia

10th International Conference on Applied Energy (ICAE2018), 22-25 August 2018, Hong Kong, China

Modeling and simulation for photoelectrochemical CO_2 utilization

Xiaojiao Luo[b], Jin Xuan[a], Eva Sanchez Fernandez[b] and M. Mercedes Maroto-Valer[b]*

[a]*Loughborough University, LE11 3TU, Loughborough, United Kingdom.*

[b]*Research Centre for Carbon Solutions (RCCS), Heriot-Watt University, EH14 4AS, Edinburgh, United Kingdom*

Abstract

A two-dimensional numerical model for a photoelectrochemical (PEC) cell.for CO_2 utilization and fuel production was developed using COMSOL Multiphysics and validated with published experimental data. The model couples computational fluid dynamics with electrochemical kinetics to account for the complex interactions inside the PEC driven by light absorption operating at the Shockyley-Queisser limit. Charge and species conservation, fluid flow and electrochemical characteristics are studied. The flow rate of CO_2 is found to be the factor affecting the cell performance. Parametric study for operating conditions is necessary in future work.

Keywords: PEC cell, CO_2 utilization, model, operating conditionsIntroduction

1. Introduction

A solar-driven photoelectrochemical CO_2 reduction system combined with electrocatalysts in contact with electrolyte can generate a variety of organic compounds, such as methane, formic acid, carbon monoxide and so on [1]. This process is a promising way for utilization of CO_2, resulting in reduction of greenhouse emissions, whilst directly producing fuels from sunlight. An increasing number of studies have been reported on this research area in recent years [2-4].

* Corresponding author. Tel.: +44 (0)131 451 8028
E-mail address: m.maroto-valer@hw.ac.uk

10.1016/j.egypro.2019.01.213

The continuous flow cell with gas diffusion electrode has been proved to enhance the performance of electrochemical and PEC system for CO_2 reduction [1, 5]. The flow PEC system could minimize mass transport limitations, improve the availability of the three phase interfaces and then solve the issue of low CO_2 solubility in aqueous[1]. Among different types of PEC systems, photoanode-driven PEC cells have a two-step process: (1) the photoanode absorbs incident light and generate electron-hole pairs. Holes on the surface of the semiconductor allow the water oxidation at the photoanode. (2) Photogenerated electrons reach the cathode through the external circuit and participate in CO_2 reduction reactions.[6] The concept of a continuous flow photoanode-driven electrochemical cell for CO_2 reduction has been experimentally demonstrated[1]. Organic fuels can be continuously produced with the consumption of CO_2. Although a large number of studies have reported PEC CO_2 utilization, modeling efforts of PEC cells for CO_2 utilization are limited. To the best of our knowledge, no work has been reported to give a theoretical study on the continuous flow PEC cell for CO_2 reduction. In this work, a mathematic model is therefore developed to achieve an understanding of the fundamental processes and focus on the optimization of the whole system performance.

2. Methodology

2.1. Model description

A 2-D numerical model was developed using COMSOL Multiphysics 5.2. The model couples computational fluid dynamics with electrochemical kinetics and semiconductor photocatalysis to analysis the PEC performance. The PEC configuration is shown in Fig. 1, which had been experimentally investigated by Erdem Irtemn et al. [1]. The PEC cell consists of two electrodes and an ionic transport membrane divided the cell into two separated anodic and cathodic compartments. As shown in Fig. 1, the cell has three inputs (catholyte, anolyte and CO_2) and two outputs (anolyte, and catholyte). Catholyte (0.5M $NaHCO_3$) and anolyte (0.5M NaOH) flows through two separated channel. TiO_2 prepared on FTO substrates has been used as photoanode material. The cathode is gas diffusion electrode made of carbon paper with a layer of catalyst on it. Therefore, it is reasonable to treat the cathode as porous medium. Electrochemical reactions are assumed to occur at the gas liquid interface in the porous cathode. The geometric parameters of PEC cell are from experimental study[1] and summarized in Table 1.

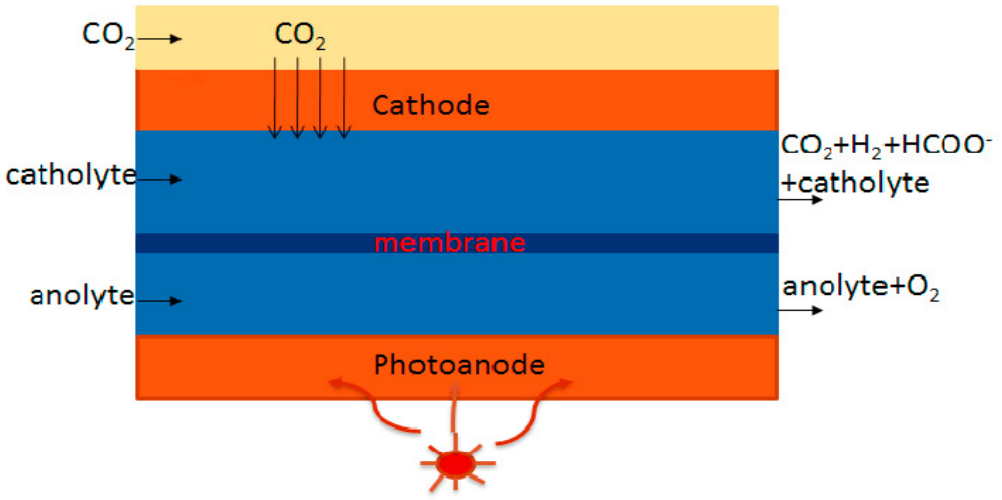

Fig.1. Schematic diagram of the PEC configuration

Table 1 Geometric parameters of the PEC cell to be modeled

Parameter	Value
Light intensity, I(100 mW cm^{-2})[1]	1 sun
Electrolyte channel height (mm)[1]	1.5
Electrolyte channel length (mm)[1]	30
GDE thickness (mm)[1]	0.3
CO2 channel height(mm)[1]	1.5

2.2. Governing equations

For the PEC to reduce CO_2 to formic acid, the half-reactions at the cathode are:

$$CO_2+H_2O+2e \rightarrow HCOO^- + OH^- \quad (1)$$
$$2H_2O + 2e \rightarrow H_2 + 2OH^- \quad (2)$$

At the anode :

$$2OH^- \rightarrow 0.5O_2 + H_2O + 2e^- \quad (3)$$

The current-voltage behavior of the photoanode was obtained from the Shockley-Queisser model fitted with the ideal diode relationship:

$$i = i_I - i_d\{\exp\left[\frac{q(V+iR_S)}{kT}\right] - 1\} \quad (4)$$

where i_I is the light generated current, id is the dark saturation current, Rs is the series resistance. The electrolyte and electrodes were assumed not to disturb the spectral absorption here, this has been proven by previous study[7]. We neglected the light scattering by the bubbles and assumed no bubbles blocked the catalytically active area or change the effective electrolyte conductivity.

The transport of electrons and holes was described by Ohm's Law:

$$i_s = -\sigma_s \nabla \emptyset_s \quad (5)$$

where is is the current density and σ_s is the electrical conductivity. For the boundary conditions, we assumed insulation at the electrolyte outer boundaries, a grounded cathode and current continuity at the electrolyte- separator interface. The electrocatalytic reactions at the electrolyte-electrode interface are modeled using Butler-Volmer relation:

$$i = i_0[\exp\left(\frac{\alpha_a F\eta}{RT}\right) - \exp\left(-\frac{\alpha_c F\eta}{RT}\right)] \quad (6)$$

with exchange current densities, i_0, anodic charge transfer coefficient, α_a, and cathode charge transfer coefficient. The overpotential is define as

$$\eta = \emptyset_s - \emptyset_1 - \emptyset_0 \quad (7)$$

where $\emptyset_s$ is the corresponding electric potential, $\emptyset_1$ the electrolyte potential, and $\emptyset_0$ is the equilibrium potential.

The steady-state governing conservation and transport equations for both neutral and charge species were given by Nernst-Planck equation[8] under the dilute-solution theory assumption[8].

$$N_i = -D_i \nabla c_i - z_i \mu_i F c_i \nabla \emptyset_1 + v c_i \tag{8}$$

where $\emptyset_1$ is the electric potential, v the velocity, c_i the concentration, D_i the diffusion coefficient, z_i the charge number, μ_i the mobility ions, and N_i the molar flux of the species.

The velocity term accounts for fluxes resulting from convective flow due to a pressure gradient, which were determined by solving the mass and laminar flow conservation equations[9]

$$\frac{\rho}{\varepsilon} u . \nabla \frac{u}{\varepsilon} = -\nabla p + \frac{\mu}{\varepsilon} \nabla u - \frac{\mu}{K} u \qquad \nabla . u = 0 \tag{9}$$

where ρ, ε, p, μ and K are the density, porosity, pressure, viscosity and the permeability respectively.

Due to the sweep-away effect of the flowing electrolyte, the assumption that the fluid inside the gas diffusion electrode is a single-phase gas flow in a porous medium is reasonable. The Darcy's law and volume-average treatment are applied on GDE region[10].

$$\nabla . (\rho \gamma u) = S_m \tag{10}$$

$$\nabla . (\rho \gamma u u) = -\gamma \nabla p + \nabla . \gamma \tau + \rho g - \left(\frac{\mu u}{K}\right) \tag{11}$$

$$\nabla . (\rho \gamma u Y_i) - \nabla . \left(\rho \frac{\gamma}{\lambda} D_i \nabla Y_i\right) = 0 \tag{12}$$

with porosity γ, tortuosity λ, and permeability K.

2.3. Boundary conditions

Since the photoanode is expected to deliver a uniform flux of holes and electrons, a constant photocurrent density was assumed at the electrode boundaries. The cathode was set to an arbitrary potential of 0 V. Hydrogen concentration is zero in the anode chamber and oxygen is zero in cathode chamber. The remaining boundaries were walls, for which a no-slip velocity condition was assumed, constant inlet velocity and constant outlet pressure.

A commercial finite-element solver Comsol Multiphysics is used to solver the coupled equations with the corresponding boundary conditions. Mesh convergence and iteration independence were attained for mesh element numbers of 10000 (small dimensions) up to 7200000 (large dimensions).

3. Results and discussion

3.1. Model validation

The model was validated by comparing the results of current density at different potentials with experiment results from literature[1]. Fig. 2(a) illustrates the comparison of the cathode performance under 1 sun illumination. The modeling results agreed well with experimental results, and therefore confirming the model validation. Fig. 2(b) shows the cathode potential and its variation as a function of the illumination intensity. The surface potential on cathode is determined by the overall transport losses, the current-voltage characteristics of the photoanode and the behavior of the catalyst. The spatial variation in the potential of the cathode produced a variation product distribution along the light intensity.

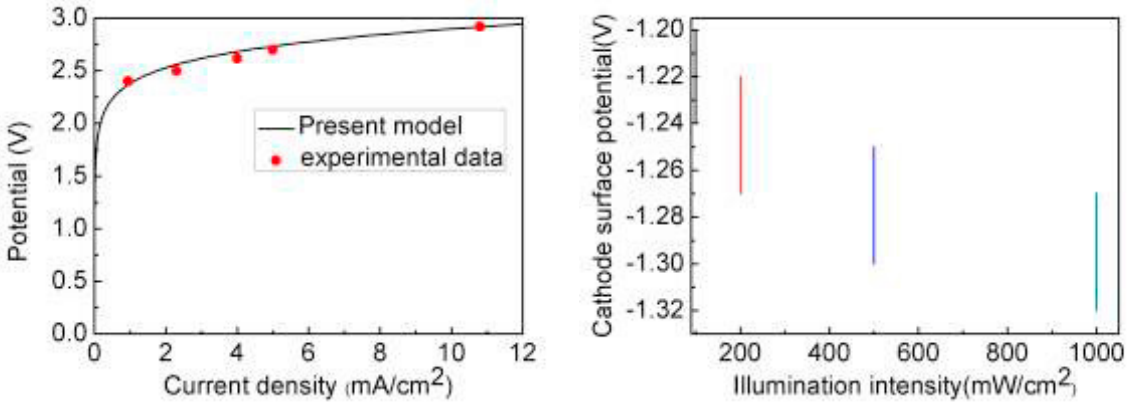

(a) (b)

Fig.2.(a) Current density at different cell voltage versus experimental data[1] under 1 sun illumination.(b) Cathode surface potential at 40 mW/cm^2 (black line), 60 mW/cm^2 (red line), 80mW/cm^2 (blue line) and 100mW/cm^2 (green line) light intensity.

Fig. 3 shows the flow rate and concentrations of CO_2 and H_2 distributions inside the gas channel. CO_2 will be consumed and its concentration will decrease along the channel. The H_2 gradually increases along the flow direction as they are generated in the photoelectrochamical reaction.

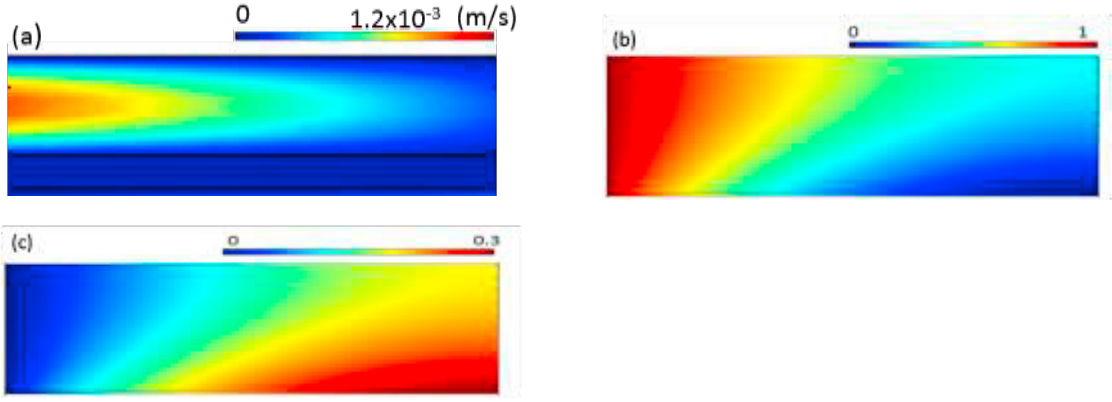

Fig. 3 (a) flow velocity, (b) mass fraction of CO_2, (c) mass fraction of H_2 inside the gas channel and at the PEC cathode .

3.2. Effect of CO_2 flow rate

In Fig. 4 (a) the current density as a function of CO_2 flow rate under 100 mW/cm^2 illumination is shown. The current density which translates into fuel production rate increases with increasing CO_2 flow rate. Fig. 4(b) illustrates the dependence of the CO_2 conversion efficiency on the CO_2 flow rate. Increase of the CO_2 flow rate will give a lower reactant conversion. So it can be found there is a trade-off between the current density and CO_2 conversion efficiency with the increase of the CO_2 flow rate. An increase of CO_2 flow rate can improve the current density, but also it would reduce the reactant conversion efficiency. From the aspects of PEC CO_2 reduction, the current density which changes to fuel production rate is a major concern and the lower CO_2 conversion pose no significant effect on PEC performance, then the higher CO_2 flow rate is preferred. If we think about the reactant utilization, the CO_2 conversion efficiency becomes the most important indicators PEC performance and the PEC cell would be requested to operate with relatively lower CO_2 flow rate. Thus, further study should be taken to optimization the operating conditions to achieve a balance point between current density and CO_2 conversion efficiency.

(a) (b)

Fig. 4 Effect of CO2 flow rate on (a) the current density and (b) faradaic efficiency under 1 sun illumination

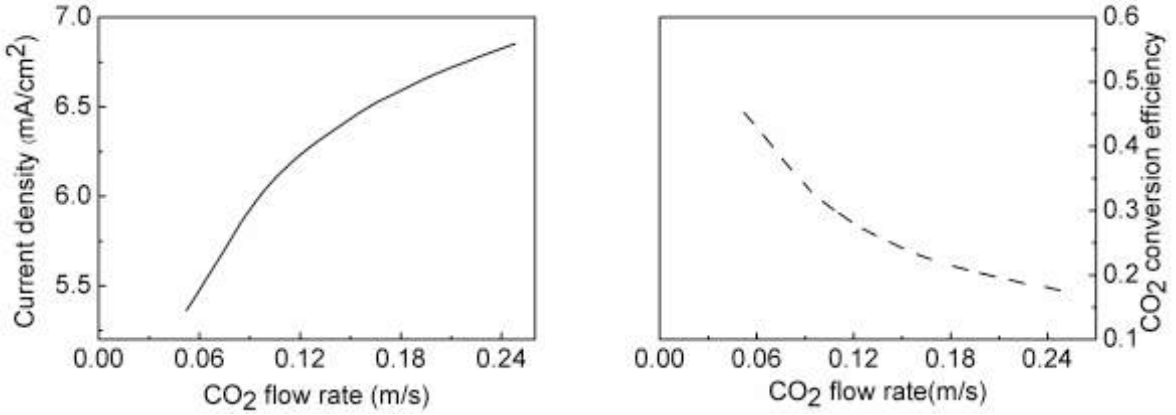

4. Conclusions

In this work, a validated model multi-physics, multi-phase (gas, solid and liquid phases) model has been developed to couple charge and species transport, fluid flow and electrochemical reactions. The effect of CO_2 flow rate on the current density and CO_2 conversion efficiency have been studied. The cathode potential will depend on the illumination intensity. Further parametric studies on the cell design and operating conditions are currently investigated, including the effect of PH of the electrolyte, electrode dimensions and separator porosity on system performance.

5. Acknowledgements

The authors thank the financial support provided by the Engineering and Physical Sciences Research Council (EP/K021796/1 and EP/R012164/1) and the Research Centre for Carbon Solutions (RCCS) at Heriot–Watt University.

Reference

[1] Irtem E, Hernández-Alonso MD, Parra A, Fàbrega C, Penelas-Pérez G, Morante JR, et al. A photoelectrochemical flow cell design for the efficient CO2 conversion to fuels. Electrochim Acta. 2017 2017/06/20/;240:225-30.

[2] Magesh G, Kim ES, Kang HJ, Banu M, Kim JY, Kim JH, et al. A versatile photoanode-driven photoelectrochemical system for conversion of CO2 to fuels with high faradaic efficiencies at low bias potentials. J Mater Chem A. 2014;2(7):2044-9.
[3] Peng Y-P, Yeh Y-T, Shah SI, Huang CP. Concurrent photoelectrochemical reduction of CO2 and oxidation of methyl orange using nitrogen-doped TiO2. Applied Catalysis B: Environmental. 2012 2012/07/23/;123-124:414-23.
[4] Satoshi Y, Masahiro D, Yuji Z, Reiko H, Hiroshi H, Yuka Y, et al. Photo-induced CO 2 Reduction with GaN Electrode in Aqueous System. Applied Physics Express. 2011;4(11):117101.
[5] Wang H, Leung DYC, Xuan J. Modeling of a microfluidic electrochemical cell for CO2 utilization and fuel production. Applied Energy. 2013 2013/02/01/;102(Supplement C):1057-62.
[6] Kalamaras E, Maroto-Valer MM, Shao M, Xuan J, Wang H. Solar carbon fuel via photoelectrochemistry. Catal Today. 2018 2018/03/10/.
[7] Döscher H, Geisz J, Deutsch T, Turner J. Sunlight absorption in water–efficiency and design implications for photoelectrochemical devices. Energy Environ Sci. 2014;7(9):2951-6.
[8] Newman J, Thomas-Alyea K. Infinitely Dilute Solutions, Electrochemical Systems. John Wiley & Sons, Inc., Hoboken, NJ, USA; 2004.
[9] Ferziger JH, Peric M. Computational methods for fluid dynamics: Springer Science & Business Media; 2012.
[10] Zhang Y, Pitchumani R. Numerical studies on an air-breathing proton exchange membrane (PEM) fuel cell. Int J Heat Mass Transf. 2007;50(23-24):4698-712.